Chlorophyll Excitations in Photosystem I of *Synechococcus elongatus*

Ana Damjanović,[†] Harsha M. Vaswani,[†] Petra Fromme,[‡,§] and Graham R. Fleming*[,†]

Department of Chemistry, University of California, Berkeley, and Physical Biosciences Division, Lawrence Berkeley National Laboratory, Berkeley, California 94720, Max-Volmer-Laboratorium für Biophysikalische Chemie and Biochemie, Technische Universität Berlin, Berlin, Germany, and Department of Chemistry and Biochemistry, Arizona State University, Tempe, Arizona 85287-1604

Received: April 11, 2002; In Final Form: July 5, 2002

The Q_y excitation energies of the 96 chlorophyll molecules in photosystem I of *Synechococcus elongatus*, both in and out of their protein environments, were obtained by using the semiempirical INDO/S method and the crystal structure geometries. The dipole−dipole approximation was used to calculate the coupling between the Q_y states of chlorophylls; in the case of closely separated chlorophylls INDO/S dimer calculations were used to determine the couplings. The effective Hamiltonian for chlorophyll Q_y excitations was constructed, enabling tentative assignment of red chlorophylls and calculation of the absorption spectrum of PSI.

Introduction

Oxygenic photosynthetic organisms fuel their metabolism with photons absorbed by two large membrane protein complexes: photosystem I (PS-I) and photosystem II (PS-II). Chlorophyll and carotenoid molecules associated with PS-I and PS-II are responsible for light absorption. The energy from absorbed photons is transferred, in the form of carotenoid and chlorophyll electronic excitations, to specialized chlorophyll molecules. These chlorophylls are referred to as P700 (in PS-I) and P680 (in PS-II), according to their absorption maxima (in nanometers). When excited by light P700 and P680 lose an electron, which travels across the membrane via a number of cofactors associated with the photosystems. The initial electron transfer in photosystems triggers a series of reactions, which result in the generation of a transmembrane proton gradient. The electrochemical and proton gradient are prerequisites for synthesis of ATP and reduction of $NADP^+$.

Understanding the molecular details of these energy and electron-transfer reactions has been precluded by a lack of atomic level structural information of PS-I and PS-II. Recently, a high-resolution crystal structure of PS-I of cyanobacterium *Synechococcus elongatus (el.)* has been reported.[1] The structure, shown in Figure 1, revealed the positions of 96 chlorophyll (Chl) and 22 carotenoid molecules. While all of these molecules are involved in light harvesting, the central six Chls are involved in electron-transfer reactions as well. The latter Chls are displayed in Figure 2. Other cofactors, two phylloquinones and three Fe_4S_4 clusters, are part of the electron-transfer chain. All of these molecules are held in place by the 12 main protein subunits, other smaller subunits, and a phospholipid. Additional cofactors, 201 water molecules, four lipids, and a putative Ca^{2+} ion, are resolved in the structure.

The electron-transfer cofactors are arranged in two groups, the so-called A and B branches, which are related by a pseudo C_2 rotational symmetry axis[1] (see Figure 2). There is a debate as to whether both branches[2] or only one[3] is involved in electron transfer. Asymmetry between the two branches begins at the P700 chlorophyll heterodimer. The B branch of P700 (P_B) is a Chl*a*, while its counterpart in the A branch (P_A) is a Chl*a*' molecule, a C13[2] epimer of Chl*a*.[1,4] However, the absorption properties of Chl*a* and Chl*a*' are identical in organic solvents,[5] suggesting that the mere presence of Chl*a*' is unlikely to induce the asymmetry in electronic properties of P700.

Interestingly, the crystal structure reveals an asymmetry in the binding environment of the P700 heterodimer; while there are a number of hydrogen bonds to Chl*a*', there are none to Chl*a*. It remains to be studied, either through mutagenesis or quantum chemistry, whether these hydrogen bonds play a role in directing the flow of electrons. Asymmetries between A and B counterparts of the remaining electron-transfer cofactors could also influence the directionality of electron flow.

Ninety Chls (shown in gray in Figure 1), whose role is to increase the effective cross-section for light absorption, surround the six reaction center Chls (shown in black). Most of the light-harvesting Chls are located at least 20 Å away from the reaction center Chls. However, two light-harvesting Chls are located at about 14 Å from the reaction center Chls. It has been suggested that they serve as bridges in transferring energy from the remaining antenna Chls to the reaction center.[6,7]

Spatial separation of most of the light-harvesting Chls and the reaction center Chls should have a signature in the energy transfer times; at least two time scales should be present, a fast one for equilibration between closely spaced bulk antenna Chls and a slow one for energy transfer between the bulk and the reaction center Chls. The well-studied system of the more simple purple bacterial reaction center surrounded by a ring-like structured antenna of bacteriochlorophylls displays two such distinct equilibration time scales.[8−10]

However, time-resolved spectroscopic studies have indicated at least three different time scales (of approximately 400 fs, 4 ps, and 40 ps) of energy equilibration in PS-I.[11,12] The 400-fs time scale is attributed to spectral equilibration between the bulk antenna Chls, while the 40-ps component is attributed to trapping by the RC. The 4-ps energy transfer time scale is attributed to energy equilibration between bulk Chl and red-shifted Chls in the antenna of PS-I.

Indeed, the PS-I absorption spectrum in the Q_y region is highly heterogeneous.[13] Most of the chlorophylls absorb between

[†] University of California and Lawrence Berkeley National Laboratory.
[‡] Technische Universität Berlin.
[§] Arizona State University.

10.1021/jp020963f CCC: $22.00
Published on Web 09/10/2002

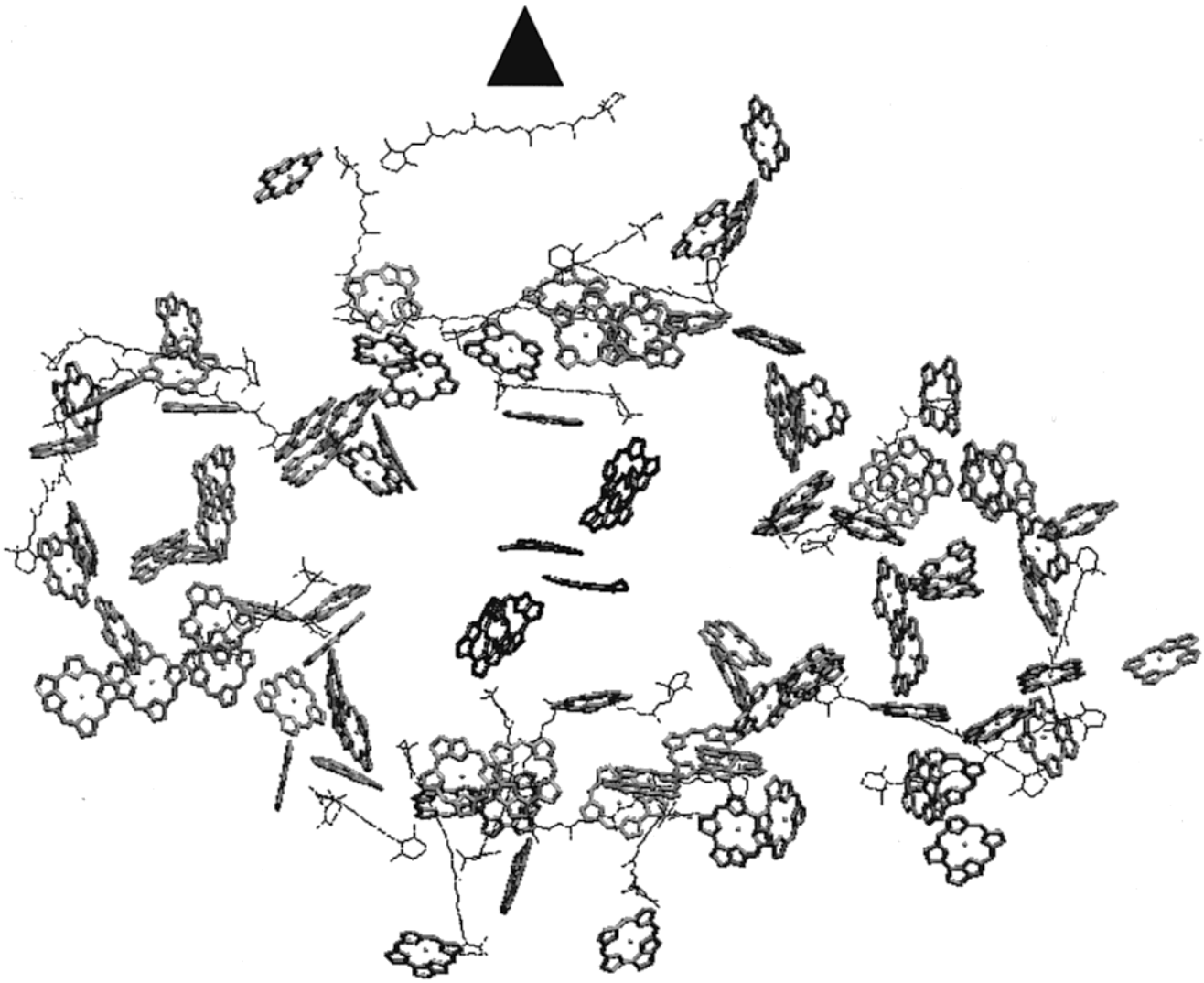

Figure 1. Location of chlorophyll and carotenoid molecules in PS-I (pdb entry 1JBO).[1] Carotenoids are shown with a thin black line. Chls are shown in gray, except for the six Chls belonging to the electron-transfer chain, which are in black. For clarity, we represent the Chl molecules by Mg−chlorin rings, lacking the phytyl chain.

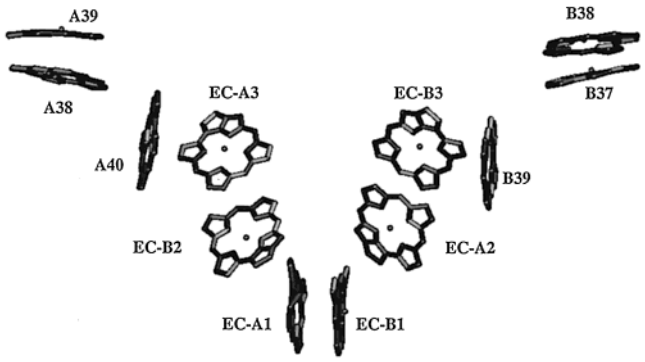

Figure 2. Chls belonging to the electron-transfer chain (EC-A1−A3, EC-B1−B3), together with the bridging Chls (A40, B39), and nearby antenna Chls (A38, A39, B37, B38). The figure displays the organization of the Chls into the A and B branches related by the pseudo C_2 symmetry axis.

660 and 680 nm, i.e., higher in energy than the P700 heterodimer. However, absorption peaks, attributed to the so-called red chlorophylls, are detectable at energies lower than 700 nm. In PS−I of *Synechococcus el*., three pools of red chlorophylls exist: a 708-nm pool, present in both monomeric and trimeric PS-I; a 715-nm pool and a 719-nm pool, both present only in PS-I trimers.[13,14] The respective absorption wavelengths refer to a low-temperature spectrum; at room temperatures these pools are blue-shifted to 702 and 708 nm, respectively.[13]

The presence and function of red chlorophylls is puzzling. On one hand, they enlarge the spectral cross-section for light absorption which might be evolutionarily advantageous.[15] On the other hand, they could reduce the overall efficiency of electron transfer, since they are located energetically below the P700 dimer. The authors of ref 16 monitored charge separation yields in PS-I particles of *Synechococcus el*. following excitation of red chlorophylls. While at room temperature the overall charge separation efficiencies remain unaffected by excitation in the red chlorophyll region, at 5 K these efficiencies are reduced, indicating that a part of the excitation energy is trapped on the red chlorophylls.[16] The red Chls could serve as traps at room temperature and undergo phonon-assisted transfer to the RC.

The spatial location and exact number of the red chlorophylls within the PS-I structure is not known. In ref 17 it was suggested, based on estimates of oscillator strength, that PS-I of *Synechococcus el*. contains about four to five pigments absorbing at 708 nm and five to six pigments absorbing at 719 nm. Hole-burning experiments on PS-I of *Synechocystis* sp. PCC 6803 and its mutants[18] and of *Synechococcus el*.[14] have

suggested that the longer wavelength absorbing red chlorophylls are associated with strongly coupled Chls (trimer absoring at 708 nm, dimer absorbing at 715 nm, and another dimer at 719 nm) with a significant charge-transfer character. They also suggest that these Chls are bound to the PsaA or PsaB subunits and are located close to the interfacial region between the PsaA/B subunits and the L and M subunits.

The red shifts could be induced either through strong couplings between the Chls or through interactions with the protein, carotenoid, or water molecules. The authors of ref 1 have suggested, based on the crystal structure of PS-I, that excitonic interactions between strongly coupled Chls are the most likely cause for this shift. Furthermore, they singled out three Chl dimers and one trimer in the PS-I structure as putative candidates for the red Chls. The 719-nm pool of red Chls is thought to be located in the trimerization region, since it is present in trimer PS-I particles and absent in PS-I monomers.

Thus, PS-I poses several intriguing questions. Where and how many red chlorophylls are there? What is their role in energy transfer? Do the two antenna chlorophylls found closest to the reaction center play a major role in connecting the antenna to the primary electron donor? Are both the A and B branches involved in electron transfer? All of these questions can now be addressed through structure-based calculations.

The goal of this paper is to estimate, through quantum chemical calculations, chlorophyll spectral shifts induced by the surrounding protein, water, or carotenoid residues or by chlorophyll−chlorophyll interactions. Based on these calculations and an effective Hamiltonian approach we will discuss the PS-I absorption spectrum and address some of the questions posed above.

Theory and Methods

In this section we will describe how the effective Hamiltonian for the Q_y excitations of the 96 Chls in PS-I is constructed. In addition we provide details of the calculations of the Chl Q_y excitation energies and couplings, through the semiempirical INDO/S method.

Effective Hamiltonian for 96 Chls of PS-I. The Chl effective Hamiltonian is expressed in the basis of single Q_y excitations

$$|i\rangle = \psi_1(g)\psi_2(g)...\psi_{i-1}(g)\psi_i(Q_y)\psi_{i+1}(g)...\psi_N(g) \qquad (1)$$

where $\psi_1(g)$ describes the first chlorophyll in the electronic ground state and $\psi_i(Q_y)$ describes the ith chlorophyll in the Q_y excited state. N is the total number of Chls, i.e., 96. The states $|i\rangle$ fulfill the orthogonality condition $\langle i|j\rangle = \delta_{ij}$.

In this basis set, the effective Hamiltonian $\hat{H}$ can be written as a 96 x 96 matrix whose diagonal matrix elements are expressed as

$$\langle i|\hat{H}|i\rangle = \epsilon_i \qquad (2)$$

Here ϵ_i is the Q_y excitation energy of Chl i. The diagonal matrix elements of the Hamiltonian $\hat{H}$ are calculated through the INDO/S method, based on the crystal structure geometries, as described further below.

The off-diagonal matrix elements

$$\langle i|\hat{H}|j\rangle = v_{ij} \qquad (3)$$

represent the couplings between chlorophyll Q_y excitations. When the separation between Chls i and j is larger than the size of the Chls, v_{ij} can be expressed as a transition dipole−transition dipole coupling, v_{ij}^{dd}, expressed (in units of cm^{-1})[19]

$$v_{ij}^{dd} = \frac{5042}{n^2}\left(\frac{\vec{d}_i\cdot\vec{d}_j}{r_{ij}^{3}} - \frac{3(\vec{r}_{ij}\cdot\vec{d}_i)(\vec{r}_{ij}\cdot\vec{d}_j)}{r_{ij}^{5}}\right) \qquad (4)$$

Here $\vec{r}_{ij}$ is a vector connecting the centers of chlorophylls i and j, expressed in angstroms. The value of the dielectric constant of the protein, n^2, is set to 1. Vector $\vec{d}_i$ describes the Q_y transition dipole moment of Chl i in a medium with dielectric constant $n^2 = 1$. With $n = 1$, the results of ref 20 lead to a magnitude of 4.48 D. This value was used in our calculations.

Due to the protein's highly heterogeneous nature, it is an oversimplification to describe the protein with a single dielectric constant or to assume that the dipole strength of all the Chls is the same. Assuming $n^2 = 1$ seems reasonable in the case of closely spaced chlorophylls. With this assumption we make errors in determination of the couplings for distant Chls; however, these errors are irrelevant for the calculations of the absorption spectrum.

We assume the direction of the vector $\vec{d}_i$ coincides with the direction connecting the NB and ND atoms of Chl i. The coordinates of those atoms are provided by the crystal structure reported in ref 1. Since the orientation of the transition dipole for emission is different from that of absorption, likely due to protein relaxation processes, the authors of ref 21 have argued that an "effective" orientation of the transition dipole moment should be used in calculations of the transition dipole−transition dipole couplings. Based on the fits of the time-resolved fluorescence anisotropy data in peridinin-chlorophyll-protein of *Amphidinium carterae*, they estimated the "effective" orientation of the Q_y transition dipoles. Our test calculations have shown that if this orientation is used instead of the orientation generated by the NB-ND direction, our results are almost identical.

When the separation between the Chls i and j is smaller than their size, the couplings v_{ij} cannot be approximated as v_{ij}^{dd}.[22−24] Several different methods have been used in the literature to estimate these couplings in purple bacterial antenna complexes.[19,22,25−29]

Model Systems and INDO/S Calculations. To calculate the chlorophyll excitation energies as well as couplings between closely spaced chlorophylls, we employed the semiempirical intermediate neglect of differential overlap method, parametrized for spectroscopy (INDO/S), together with singly excited configuration interaction (CIS) type calculations.[30,31]

The INDO/S calculations were performed on four model systems displayed in Figure 3. Those include a single chlorophyll, a chlorophyll surrounded by its neighboring residues, a dimer of chlorophylls, and a dimer of chlorophylls surrounded by its neighboring residues. Hereafter we refer to these four model systems as Chl, Chl+res, dimer, and dimer+res, respectively. Neither the chlorophyll phytyl tails nor the protein backbone atoms were included in any of the calculations. The protein and water residues included in the calculations were those that had an atom within 2.5 Å from any of the chlorophyll atoms. The "pick" criterion was applied only after hydrogen atoms were added to the structure (see next paragraph).

The crystal structure geometry[1] revealed the positions of non-hydrogen atoms only. To perform INDO/S calculations we added the missing hydrogen atoms to the crystal structure geometries with the molecular modeling program XPLOR.[32] We then minimized the positions of hydrogens with the program MOPAC, employing the PM3 semiempirical Hamiltonian.[33] Hydrogen minimizations were performed separately on each of the four model systems.

The INDO/S calculations on Chl and Chl+res systems were performed within the Gaussian 98 program,[34] including all of

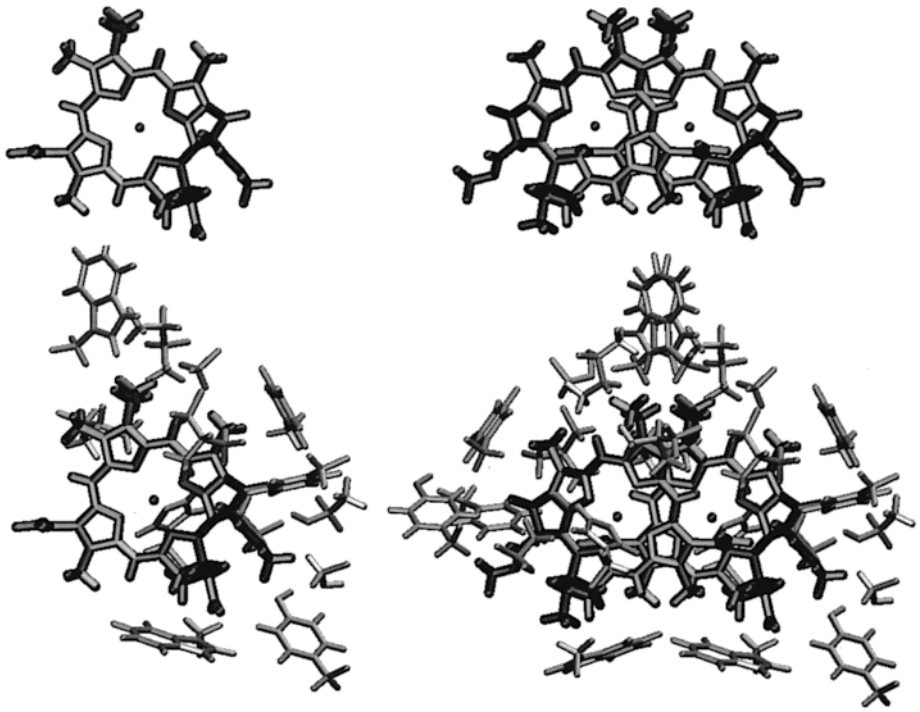

Figure 3. Model systems employed for INDO/S calculations: (top left) chlorophyll, (top right) dimer, (bottom left) chlorophyll + residues, (bottom right) dimer + residues.

the singly excited configurations, i.e., full active space. Various sizes of active space have previously been used for INDO/S chlorophyll calculations,[35,36,29] while the original parametrization performed on pyrroles included only configurations that lie up to ~75 000 cm^{-1} (mostly π-electron configurations).[30] Due to the use of a larger active space, our calculated spectrum is red-shifted compared to the experimental absorption spectum. However, we are mainly concerned with the differences in excitation energies between the 96 chlorophylls, not their absolute values. The variable number of protein residues included in the calculations of chlorophyll excitation energies (and therefore the number of atoms of the systems of study) would have significantly complicated the choice of active space if we had opted to use a reduced active space. By choosing a full active space we have consistently included all of the relevant configurations in our calculations. Our test calculations with a smaller sized active space, performed for a limited number of selected Chl+res models, resulted in differences in excitation energies of the selected chlorophylls that were very similar to the values obtained through full active space calculations, thus justifying our use of a full active space.

Due to the variable number of residues present in the dimer+res structures, we also opted to use a full active space for the INDO/S dimer and dimer+res calculations. To extract the couplings v from the dimer (dimer+res) calculations we used a dimer Hamiltonian model[28]

$$\hat{H}_{ij} = \begin{pmatrix} \epsilon_i + \lambda & v \\ v & \epsilon_j + \lambda \end{pmatrix} \tag{5}$$

Here ϵ_i and ϵ_j are monomer excitation energies as determined from the INDO/S calculations on Chl (Chl+res). λ is a shift resulting from quantum chemistry calculations on dimers and is due to mixing of excitonic and charge-transfer states. These shifts are well-known and have been discussed previously in ref 36. The eigenvalues of the dimer Hamiltonian are equal to the lowest two excitation energies as determined from INDO/S dimer calculations. Once these excitation energies, together with ϵ_i and ϵ_j, are known, the coupling v and the shift λ are easily extracted from eq 5.

To evaluate the quality of the dimer calculations, we performed an additional set of calculations with a completely different method, namely, the transition density cube (TDC) method developed by Krueger et al.[22] The couplings determined through the TDC method were scaled as described in ref 22 to correspond to the vacuum transition dipole moment of 4.48 D.[20] The scaling was included because the CIS method underlying the TDC calculations overestimates the transition dipole moment. The scaling of the total transition density (and thus the corresponding couplings) is justified if the CIS method predicts the shape of the density correctly. We argue that this is the case for two reasons: (i) The CIS method correctly predicts the direction of the transition dipole moment. This direction would have been predicted incorrectly if the shape of the transition density was wrong. (ii) An entirely different quantum chemical method, the time-dependent density functional theory method, predicts almost the same shape of the transition density as the CIS.[37]

Results and Discussion

Chlorophyll Excitation Energies. We have calculated the Q_y excitation energies for each of the 96 Chl+res model systems, as introduced in the methods section. Since the Chl+res model systems did not include carotenoid molecules, we have accounted for the carotenoid effects in the following way. Excitation energies calculated for the Chl model system (no protein residues) were compared with excitation energies determined for new, Chl+carotenoid model systems (this calculation was performed only for chlorophylls that had carotenoid residues in their neighborhood). The differences in excitation energies between Chl and Chl+carotenoid systems were then added to calculated Chl+res energies.

These results are displayed in Table 1 and Figure 4. The figure shows the location of Chl Mg atoms in the PS-I structure. The

TABLE 1: Chl Excitation Energies, As Determined from Our Calculations (in cm^{-1}) and Blue-Shifted by 830 cm^{-1} (in nm). These Energies Reflect Shifts Due to Interactions with Carotenoids but Not Due to Charge-Transfer Interactions (the Latter are Presented in Table 3)

Chl no.	energy, cm^{-1}	energy, nm	Chl no.	energy, cm^{-1}	energy, nm
EC-A1	13 201	710	EC-B1	13 964	674
EC-A2	14 105	668	EC-B2	13 787	682
EC-A3	13 744	685	EC-B3	13 863	679
A1	14 133	667	B1	13 879	679
A2	13 936	676	B2	13 658	688
A3	13 603	691	B3	13 875	679
A4	14 006	672	B4	14 328	658
A5	14 136	666	B5	13 721	686
A6	13 970	674	B6	13 801	682
A7	14 129	667	B7	13 811	681
A8	14 247	662	B8	14 237	662
A9	14 644	645	B9	13 953	675
A10	14 257	661	B10	14 271	661
A11	14 050	670	B11	13 786	682
A12	14 170	665	B12	14 186	664
A13	13 847	679	B13	13 928	676
A14	13 565	693	B14	14 216	663
A15	13 976	674	B15	13 688	687
A16	14 315	659	B16	13 871	679
A17	13 745	686	B17	13 990	673
A18	14 028	672	B18	13 872	679
A19	13 963	674	B19	13 828	680
A20	13 866	679	B20	13 774	683
A21	14 315	659	B21	14 411	654
A22	13 911	677	B22	13 796	682
A23	13 803	681	B23	14 017	671
A24	13 692	687	B24	13 648	689
A25	13 981	673	B25	13 880	678
A26	13 832	680	B26	13 302	706
A27	13 978	673	B27	14826	637
A28	14 513	650	B28	14 324	658
A29	14 695	643	B29	13 783	683
A30	13 909	677	B30	14 214	663
A31	13 640	689	B31	14 047	670
A32	14 229	662	B32	14 123	667
A33	13 847	679	B33	14 008	672
A34	13 973	674	B34	14 139	666
A35	13 687	687	B35	13 523	695
A36	13 835	680	B36	14 017	671
A37	13 999	672	B37	13 791	682
A38	14 125	667	B38	13 812	681
A39	13 644	689	B39	13 800	682
A40	13 911	677	L01	13 605	691
J01	14 100	668	L02	13 832	680
J02	14 190	664	L03	13 787	682
J03	13 990	673	M01	14 201	663
K01	14 026	671	X01	14 008	672
K02	14 131	667	PL01	14 025	671

coloring is according to calculated excitation energies of the corresponding Chl+res (+carotenoid) systems. The energies have been blue-shifted by 830 cm^{-1} in order to match the peak of the experimental spectrum. The following scheme was employed (numbers in parentheses refer to energies in nanometers): dark red (710−720), red (700−710), orange (690−700), yellow (680−690), green (670−680), light blue (660−670), dark blue (650−660), purple (630−650).

The most red Chl was found to be the epimer (P_A) in P700. The same result was obtained from calculations on Chl model systems with no protein residues, suggesting that this low energy is a result of geometric distortion of the Chl *a*′ molecule.

Mutation studies on purple bacterial light-harvesting complexes have suggested that substitutions of the hydrogen bonding residues induce blue shifts in the absorption spectrum.[38,39] A recent mutation study on the P700 dimer of PS-I in *Chlamydomonas reinhardtii*[40] finds a significant blue shift of the low energy exciton band of P700 when Thr A739, a possible hydrogen bond donor to the 9-keto group of the P_A, was mutated to Val, suggesting thus that hydrogen bonding interactions with P_A induce a large red shift in the excitation energy of this Chl. While these mutation studies might suggest that the hydrogen bonding interactions could be the source of the large red shift of the epimer excitation energy (possibly through geometric distortions induced by hydrogen bonds), our method is not capable of providing evidence for or against such a statement.

To further benchmark our estimate of the P_A excitation energy, and generally the quality of the INDO/S calculations, we performed ab initio calculations using Gaussian 98 [34] with the 3-21G* basis set on a total of $M = 19$ Chls (P_A and 18 other Chl residues). The test study was performed on Chl model systems that did not include protein or carotenoid residues. The difference between the calculated Chl energies (ϵ_i) from the meanvalue ($\bar{\epsilon} = (1/M)\sum_{i=1}^{M}\epsilon_i$) is shown in Table 2. The standard deviations of the distributions of $\Delta\epsilon_{\mathrm{INDO/S}} = \epsilon_{\mathrm{INDO/S}} - \overline{\epsilon_{\mathrm{INDO/S}}}$ and $\Delta\epsilon_{3-21G^*} = \epsilon_{3-21G^*} - \overline{\epsilon_{3-21G^*}}$ are 221 and 210 cm^{-1}, respectively. The mean value of the absolute error $|\Delta\epsilon_{\mathrm{INDO/S}} - \Delta\epsilon_{3-21G^*}|$, as estimated from the comparison of the two methods, is about 50 cm^{-1}, i.e., smaller than the standard deviation of the distribution.

The test calculation indicates that both quantum chemistry methods place the excitation energy of the epimer P_A much lower than the energy of any other Chl. Furthermore, except for a few Chls, the $\Delta\epsilon$ values compare rather well between the two methods, suggesting that the trends found in our INDO/S calculations can be trusted.

To study the effects of various protein residues on Chl excitation energies we compared excitation energies calculated with and without the protein residues. Charged residues had by far the most drastic effect; most of the chlorophylls for which we observed a shift larger than 323 cm^{-1} had a charged residue nearby. Furthermore, the direction and magnitude of the shift could be correlated with the charge and location of the residue.

Hanson et al. have extensively studied electrochromic effects in bacteriochlorophyll through INDO calculations.[41] They concluded that the direction of the shift of the Q_y excitation energies could be related to the location and sign of the charge placed in the vicinity of bacteriochlorophyll; positive charges placed near ring I (near the NB atom) or negative charges placed near ring III (near the ND atom) resulted in red shifts, whereas reversed charges at these locations caused blue shifts. The trends observed in our calculation agree well with the conclusions in ref 41. Using their findings, the authors of ref 41 were able to rationalize spectral shifts of the accessory BChls following primary charge separation in the photosynthetic reaction centers of purple bacteria.

A large red shift was also observed for Chl A14 (the Chl labeling scheme follows that of ref 1), even though this Chl does not have charged residues in its vicinity. In this case the shift is due to the presence of an aromatic residue, histidine, located 3.6 Å from and parallel to the Chl pyrrole ring III. Our test calculations showed that this histidine produced a red shift of about 18 nm.

In connection with this Chl residue (A14) we point out a possible source of error in our calculations. This error could stem from the assumed protonation state of the histidine residue. Determination of the protonation state of histidine is beyond the scope of this manuscript. For simplicity we have assumed that all of the histidines are in their neutral state. This assumption is plausible for all of the histidines that are ligated to Chls (which is the large majority), since one would expect that no H atoms

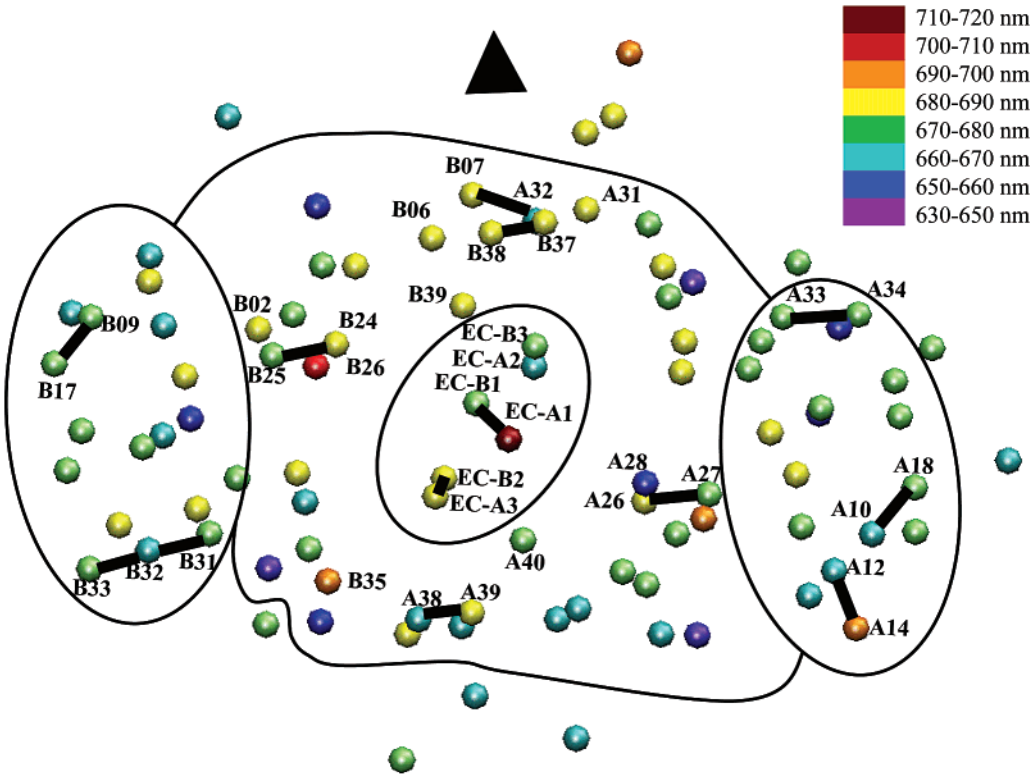

Figure 4. Mg atoms of the Chl molecule in PS-I viewed along the membrane plane. The coloring is according to calculated excitation energies, as described in the text. From red most to blue most Chls, the color codes are as follows: dark red (EC-A1 only), red, orange, yellow, green, light blue, dark blue, purple. Chlorophylls with the strongest dipole−dipole couplings are connected by black bars. The black triangle shows the trimerization axis. The black lines separate the following regions: the reaction center, the central antenna, and the two peripheral antennae.

TABLE 2: Comparison of the INDO/S Method with the 3-21G* ab Initio Calculations[a]

Chl	$\Delta\epsilon_{\mathrm{INDO/S}}$	$\Delta\epsilon_{3-21G^*}$	Chl	$\Delta\epsilon_{\mathrm{INDO/S}}$	$\Delta\epsilon_{3-21G^*}$
EC-A1	778	669	A39	88	168
EC-A2	318	397	B07	105	98
EC-A3	17	47	B09	128	199
EC-B1	51	43	B17	29	109
EC-B2	51	3	B31	178	98
EC-B3	76	144	B32	56	20
A32	74	136	B33	91	55
A33	30	40	B37	156	108
A34	31	28	B38	175	152
A38	145	108			

[a] We are interested in the distribution of calculated energies from the mean value, not the absolute values of the calculated energies, therefore we only show $\Delta\epsilon_{\mathrm{INDO/S}} = \epsilon_{\mathrm{INDO/S}} - \overline{\epsilon_{\mathrm{INDO/S}}}$ and $\Delta\epsilon_{3-21G^*} = \epsilon_{3-21G^*} - \overline{\epsilon_{3-21G^*}}$. Here $\epsilon_{\mathrm{INDO/S}}$ and ϵ_{3-21G^*} are the calculated energies for 19 chosen Chls (see the Chl labels in the table), and $\overline{\epsilon_{\mathrm{INDO/S}}}$ and $\overline{\epsilon_{3-21G^*}}$ are their respective average values, as defined in the text.

are found between the coordinating N atom of histidine and the Mg atom of chlorophyll. However, in the case of chlorophyll residue A14 it is not clear what the protonation state of the histidine is. A test calculation shows that a positively charged histidine would cause a blue shift of 16 nm instead of the 18-nm red shift induced by a neutral histidine.

We find that spectral shifts induced by the carotenoid molecules are small. For only five Chls we observed a shift greater than 100 cm^{-1}; however all the calculated shifts are smaller than 160 cm^{-1}. This also suggests that the chlorophyll phytyl tails would have only affected our results slightly had we included them in our calculations.

Couplings. To find out which Chl dimers might be candidates for the red Chls, we calculated the dipole−dipole couplings between all of the Chls, according to eq 4, and employing $n = 1$. We chose $n = 1$ instead of the standard of $n = 1.33$ in protein because the excitonically coupled chlorophylls do not have much protein separating them. This also enables us to compare the dipole−dipole couplings to the in vacuo calculated INDO/S dimer couplings (see Table 3). All the dimers that had couplings larger than 100 cm^{-1} are indicated by means of a connecting black bar in Figure 4. For the selected dimers we determined the couplings through the INDO/S dimer method (see theory and methods section), as well as through the transition density cube (TDC) method.[22]

Table 3 compares the couplings calculated through the following methods: INDO/S dimer+res; INDO/S dimer (no residues), TDC, dipole−dipole calculation according to eq 4, TDC dipole−dipole calculations. The TDC dipole−dipole couplings are also obtained through eq 4 (taking $n = 1$), only now the directions of the transition dipole moments are obtained through the TDC method[22] (instead of taking the direction defined by the NB and ND Chl atoms) and the center of mass is calculated for every Chl geometry (instead of assuming that it is defined by the position of the Mg Chl atom). All of the couplings are in cm^{-1}. The distances (in angstroms) between the Mg atoms of the dimers are also displayed in the table.

Comparison of INDO/S dimer+res (i) and INDO/S dimer (ii) couplings in Table 3 at first suggests that protein residues either have a rather small effect on the couplings or enhance the couplings. However, it is hard to judge the protein effects on the couplings since the in vacuo couplings (ii) are obtained from crystal structure geometries, already influenced by the protein. Increase of the couplings by the medium is opposite of what would be expected from a classical electrostatic theory; indeed, eq 4 suggests a decrease in the coupling when protein effects are taken into account. However, such a model might be too simple for the confined geometry of PS-I. Hsu et al.

TABLE 3: Couplings, Distances between Mg Atoms of Chls, and Spectral Shifts

Chl dimer	dimer+r,[a (I)] cm^{-1}	dimer,[a (ii)] cm^{-1}	TDC,[a (iii)] cm^{-1}	Dd,[a (iv)] cm^{-1}	TDC(dd),[a (v)] cm^{-1}	MgMg,[b] Å	λ[c]
A32−B07	295	268	187	224	239	8.924	248
A33−A34	190	198	131	170	167	9.899	2
A38−A39	308	211	114	175	239	8.064	65
B37−B38	240	236	135	214	274	7.594	72
B09−B17	104	101	95	193	186	8.754	25
B31−B32	248	133	106	265	269	8.313	155
B32−B33	106	106	73	244	265	8.138	93
A26−A27	277	216	131	181	125	8.510	90
B24−B25	295	207	111	175	111	8.354	107
A10−A18	169	176	130	198	185	9.092	6
A12−A14	160	148	97	244	258	8.376	45
EC-A1−EC-B1	90	85	141	240	410	6.341	106
EC-B2−EC-A3	101	35	59	123	152	8.744	48
EC-A2−EC-B3	44	35	55	143	181	8.219	26

[a] Couplings calculated through the INDO/S method on the dimer+res model (i) and the dimer model (ii) and through the transition density cube method (iii). The dipole−dipole couplings calculated according to eq 4 and taking $N = 1$, as described in the theory section (iv), and through the TDC method *(v)*. [b]Distances between Mg atoms of Chls comprising the dimer. [c]Spectral shifts λ (eq 5). All the couplings are in cm^{-1}, while the distances are in angstroms.

have shown, through time-dependent density functional response theory, that the medium can either enhance or reduce the couplings between two closely spaced chromophores, depending on the orientation and alignment between the two chromophores.[42]

By comparison of the INDO/S in vacuo calculations (ii) and TDC calculations (iii), one sees that the calculated couplings can differ by as much as 45%. However, both methods have defects. While the TDC calculations neglect overlap-dependent contributions,[28] the INDO/S results depend on the size of the active space used.[30]

When the Mg−Mg distances are short, the dipole−dipole couplings calculated with methods iv and v give different results. This is due to an approximation applied in eq 4 that the center of mass coincides with the position of the Mg atom. This approximation is not applied in the case of dipole−dipole couplings calculated through the TDC method. This is as expected: at short distances the dipole−dipole approximation breaks down, while at long distances the dipole−dipole couplings calculated with the two methods agree well.

Finally we discuss the role of mixing of the excitonic and charge resonance states of the dimer. This mixing gives rise to shifts given by λ in eq 5. These shifts will be taken into account within the effective Hamiltonian model, by adding the corresponding calculated shift λ, listed in Table 3, to the excitation energies ϵ_i of every Chl comprising a dimer.

The shifts due to charge resonance interactions were discussed in detail in ref 36 for the case of the special pair in the bacterial photosynthetic reaction center. It was shown that, for this particular case, the charge resonance interactions and exciton splitting contribute equally to the red-shift of the BChl Q_y state when the special pair dimer is formed. In our calculations (Table 3) these shifts are determined to vary between almost zero (for dimer A33-A34) to about 240 cm^{-1} (for dimer A32-B07). Test calculations performed on model systems of dimers without protein residues (data not shown) indicate that the protein has a strong influence on the value of λ. The same was found in earlier studies by Thompson et al.[36] Apart from the protein effects, the shifts depend on the dimer geometry.[43]

Effective Hamiltonian. Next, we will solve the effective Hamiltonian $\hat{H}$ describing the coupled Q_y excitations between the Chls in PS-I. All the parameters for this Hamiltonian are now provided: the site energies, ϵ_i, are obtained when the INDO/S energies obtained for the Chl+res system are corrected for the shifts induced by carotenoids and for charge resonance effects; the couplings v_{ij} are calculated through INDO/S dimer+res calculations (column i in Table 3), the remaining couplings v_{ij}^{dd} are determined according to eq 4, employing $n = 1$.

The eigenenergies of the effective Hamiltonian together with the eigenstates, which we will refer to as the exciton states, reveal how the excitation energies and couplings jointly affect the PS-I spectrum. The exciton states are expressed as

$$|\tilde{n}\rangle = \sum_{i=1}^{96} c_{\tilde{n},i}|i\rangle, \qquad \tilde{n} = 1, ..., 96 \tag{6}$$

where $|i\rangle$ is given by eq 1.

We also determined the dipole strength of each PS-I excitonic state. The dipole strength $D_{\tilde{n}}$ associated with the optical transition to the state $|\tilde{n}\rangle$ is defined as the square of the transition dipole moment $\vec{d}_{\tilde{n}}$, i.e., $D_{\tilde{n}} = |\vec{d}_{\tilde{n}}|^2$. The transition dipole moment $\vec{d}_{\tilde{n}}$ of the excitonic state $|\tilde{n}\rangle$ is defined as

$$\vec{d}_{\tilde{n}} = \sum_{i=1}^{96} c_{\tilde{n},i}\vec{d}_i \tag{7}$$

where $\vec{d}_i$ is the transition dipole moment for the Q_y transition of chlorophyll i.

By examining the expansion coefficient $c_{\tilde{n},i}$ of the eigenvectors $|\tilde{n}\rangle$, information about the nature of the eigenstate can be derived. We will present the coefficients for the lowest four excitonic states. Coefficients smaller than 0.1 are not displayed.

The lowest excitonic state, determined at 13 066 cm^{-1} with a dipole strength of $1.39D_0$ (by D_0 we denote the dipole strength of an individual Chl) can be expanded as

$$|\tilde{1}\rangle = -0.98|\text{EC-A1}\rangle + 0.11|\text{EC-B1}\rangle - 0.16|\text{EC-B2}\rangle \tag{8}$$

Here $|$EC-A1$\rangle$ denotes the Q_y excitation of the Chl labeled EC-A1. This excitonic state seems to be localized 96% on the epimer P_A, only 1% on P_B, and 2% on the Chl that is the second closest to P_A.

The eigenvector corresponding to the second lowest excitonic state, absorbing at 13 289 cm^{-1} with a strength of $0.23D_0$, can be written as

$$|\tilde{2}\rangle = -0.96|\text{B26}\rangle - 0.14|\text{B24}\rangle + 0.15|\text{B07}\rangle \tag{9}$$

This excitation is localized 91% on Chl B26, 2% on Chl B24, and 2% on Chl B07. The mixing in of B07 excitation is a

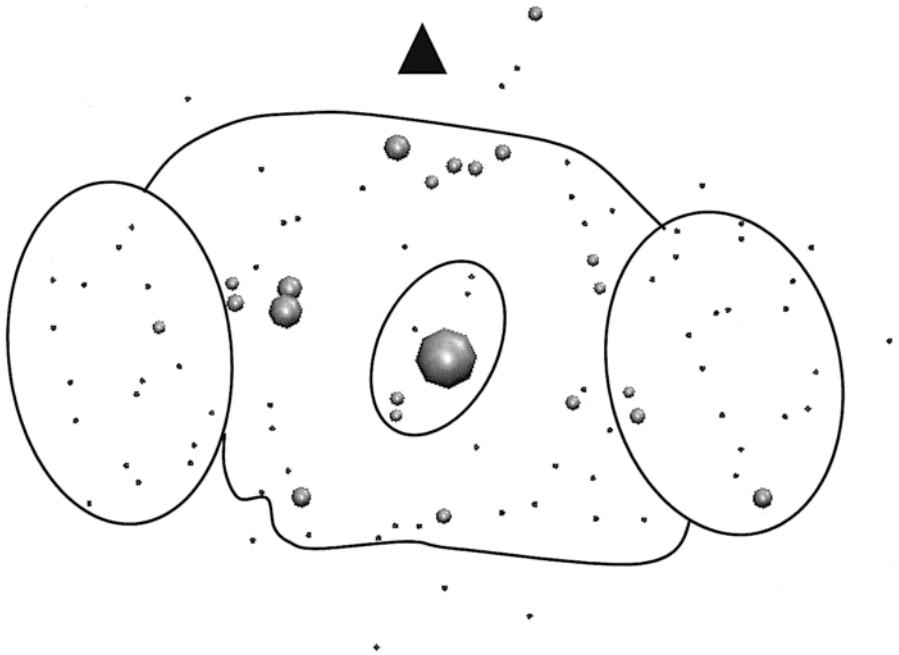

Figure 5. Boltzmann populated exciton densities. The Chls with populations larger than 1% are drawn as enlarged spheres, with the surface area of the spheres proportional to the population density.

consequence of the similarity of the energies of eigenstates $|\tilde{2}\rangle$ and $|\tilde{3}\rangle$, and it disappears when static disorder is included in our calculations.

The third lowest excitonic state, determined at 13 302 cm^{-1} with a strength of $3.15D_0$, can be expressed as

$$|\tilde{3}\rangle = 0.32|A31\rangle - 0.46|A32\rangle - 0.24|B06\rangle + 0.76|B07\rangle \quad (10)$$

This indicates that this excitonic state is delocalized over four pigments with about 10% on Chl A31, 21% on Chl A32, 6% on Chl B06, and 58% on Chl B07.

The fourth lowest excitonic state, absorbing at 13 336 cm^{-1} with a strength of $1.28D_0$, has the following coefficients

$$|\tilde{4}\rangle = -0.80|B24\rangle - 0.56|B25\rangle + 0.18|B26\rangle \quad (11)$$

This state corresponds to a dimeric state, localized 64% on Chl B24 and 31% on Chl B25, with a small admixture (3%) from Chl B26.

Boltzmann Populated Exciton Densities. The Boltzmann populated exciton density ρ_i on Chl i is defined as[44]

$$\rho_i = Z^{-1}\sum_n c_{\tilde{n},I}{}^2 \exp(-E_{\tilde{n}}/kT) \qquad Z = \sum_n \exp(-E_{\tilde{n}}/kT) \quad (12)$$

Here $E_{\tilde{n}}$ are eigenenergies of Hamiltonian $\hat{H}(2,3)$. Temperature T is set to 300 K, and k is the Boltzmann constant.

The Boltzmann populated exciton densities show which Chls would be populated at $T = 300$ K after thermal equilibrium has been achieved, assuming that the P700 heterodimer is not a sink for excitation energy. The Boltzmann populated exciton densities do not provide information about pathways or time scales of thermal equilibration. In addition, because no electron−phonon couplings are included, the possibility of time-dependent localization of the excitation is excluded in this simple calculation. The electron−phonon couplings could in principle be included through calculations based on the polaron model.[44,45]

Figure 5 and Table 4 display the Boltzmann populated exciton densities for Chls with populations greater than 1%. In the figure, these Chls are shown as enlarged spheres; the surface area of the enlarged spheres are proportional to the population densities.

TABLE 4: Boltzmann Populated Exciton Densities for Chls with Populations Greater than 1%

Chl	population	Chl	population
A27	0.0107	B37	0.0177
A24	0.0119	A39	0.0182
A35	0.0120	A3	0.0187
B15	0.0124	B25	0.0242
EC-B2	0.0126	B35	0.0288
EC-A3	0.0126	A14	0.0318
A2	0.0138	B7	0.0478
A32	0.0164	B24	0.0489
A26	0.0170	B26	0.0862
A31	0.0175	EC-A1	0.2674
L01	0.0176		

Through comparison with Figure 4 and Table 3 these populations can be readily rationalized. All of the Chls calculated to absorb at wavelengths longer than 690 nm (colored dark red, red, and orange in Figure 4) are found to have nonnegligible population density. Furthermore, Chls found to be strongly coupled to other Chls, especially Chls B24, B25, and B07, have significant population density. This was also found by Monte Carlo simulations after spectral based assignments of chlorophyll site energies in photosystem I.[46]

Role of Particular Chlorophylls. On the basis of our results for the excitation energies, couplings, effective Hamiltonian eigenstates and eigenenergies, and population densities, we can now speculate on the role of particular Chls in excitation transfer.

Reaction Center Chls. The Chl epimer, P_A, was determined to have the lowest excitation energy among the RC Chls. Furthermore, Figure 4 indicates that the excitation energies of all three RC Chls of the B-branch are higher than those of the A-branch. While this strongly suggests that excitation energy will be funneled and confined to the A-side, it cannot be taken as a proof that electron transfer occurs via the A-branch. To learn about the electron-transfer pathway, the redox properties of the RC Chls need to be determined.

The Boltzmann populated exciton densities, as well as the nature of the lowest excited state (eq 8), suggest that the excited state of the P700 heterodimer is an excited P_A monomer. This can also be concluded by comparing the energy gap between P_A and P_B ($|\epsilon_1 - \epsilon_2| \sim 726$ cm^{-1}) with the coupling between P_A and P_B ($v \sim 81$ cm^{-1}). For these values of parameters $|\epsilon_1 - \epsilon_2|$ and v, Hamiltonian $\hat{H}_{ij}$ (eq 5) has highly localized wave functions.

However, the calculated excitation energy of P_A, characterization of the P700 state as monomeric, and placement of the P700 energy below that of the red Chl states are in disagreement with the experimental absorption spectrum and the hole burning experiments,[47] which suggest that P700 is a dimer. In the methods section we have shown that two quantum chemical methods independently place the energy of P_A significantly lower than the energy of any other Chl. We therefore suggest that the origin of the low calculated energy of P_A might lie in the coordinates reported for the crystal structure.

Although several distances between electron-transfer cofactors change by 0.5−2 Å in the 2.5-Å resolution structure as compared to the 4-Å resolution structure, the decrease in the P_A–P_B spacing from 7.5 Å[6] to 6.34 Å[1] is the only one likely to perturb the nature of the electronic states significantly, since all other separations are greater than 8.2 Å. At 6.34-Å separation the degree of delocalization will depend strongly on the relative transition frequencies of Chls EC-A1 and EC-A2, and since we do not yet have an analysis of why our calculated transition energy for P_A is so low, it seems appropriate to investigate the nature of the P700 absorption if the transition frequency of P_A is artificially set so as to produce P700 absorption at 700 nm. This can be achieved by placing the P_A transition frequency at 14 349 cm^{-1}. The expansion coefficients for this state are now

$$|\mathrm{P700}\rangle = -0.78|\mathrm{EC\text{-}A1}\rangle + 0.16|\mathrm{EC\text{-}B1}\rangle - 0.37|\mathrm{EC\text{-}B2}\rangle - 0.22|\mathrm{EC\text{-}A3}\rangle \quad (13)$$

With the wave function localized 60% on |EC-A1⟩, 2.5% on |EC-B1⟩, 14% on |EC-B2⟩, and 5% on |EC-A3⟩, this state can hardly be considered monomeric. With the present information it is not possible to say if the problem with the P_A transition frequency lies in the structural information (e.g., location of H-bonding groups) or in the electronic structure calculations themselves, although the agreement between ab initio and semiempirical methods at least suggests that the latter are self-consistent.

Red Chls. Based on the red-most calculated excitonic states, we speculate on the location of the red Chls. The second lowest excitonic state (eq 9) is a monomeric excitation of Chl B26. The excitation energy of this Chl was calculated to be so low due to a red shift (of 379 cm^{-1}) induced by a neighboring aspartate residue. Surprisingly, the excitation energy of the A-branch counterpart of this chlorophyll, namely, Chl A28, was calculated to be much higher in energy.

To understand this we carefully analyzed all the residues surrounding Chls A28 and B26. Both Chls display a symmetric arrangement of a negatively charged aspartate and a positively charged arginine residues. Chl A28 has an additional arginine residue nearby, which may cause, as suggested by our calculations, a blue shift of the A28 transition compared to the B26 transition.

We note, however, that we have probably calculated the excited-state energy of Chl B26 to be lower than it actually is. This is because our criterion for including the residues in the excited-states calculations excludes the arginine residue located close to Chl B26. When we included this residue in our test calculation, the excitation energy of Chl B26 was shifted 15 nm to the blue. As a consequence, the eigenstate attributed to this Chl would not be the second lowest in energy but would still be among the five lowest energy ones.

The fourth lowest exciton state (eq 11) is a dimer of Chls B24 and B25. The red shift for this dimer may be due to strong excitonic coupling, charge resonance interactions within the dimer, and a relatively low excited-state energy of Chl B24. This dimer might be a candidate for red Chls.

The group of Chls belonging to the A-branch (A26, A27), located symmetrically to B-branch Chls B24, B25, has lower population densities and higher excitation energies than the corresponding Chls on the B-side. Table 3 indicates that the excitonic coupling and the charge resonance shift within the dimer A26−A27 was calculated to be very similar to that of its counterpart on the B-side (i.e., the dimer B24−B25). The asymmetry between the two groups thus stems from the calculated excitation energies; the excited states of Chls A26 and A27 were calculated to be higher than those of their counterparts, B24 and B25. Based on the above observations, we speculate that these two Chl dimers could be the red Chls absorbing at 708 nm (A26, A27) and 715 nm (B24, B25).

The 719-nm pool of red Chls is believed to be located close to the trimerization region. We speculate that these red Chls could be formed by the four Chls contributing to the third lowest excited state (eq 11), i.e., Chls, A31, A32, B06, and B07. The red shift of this group is caused by the strong excitonic and charge resonance interactions in the A32−B07 dimer (Table 3) and also by the dimer's relatively strong coupling to the low-energy Chls A31 and B06. This is in accord with the proposed nature (strongly coupled Chls with significant charge-transfer character) and location (toward the trimerization region but bound to PsaA and/or PsaB) of the long-wavelength Chls.[18,14]

Finally, we compare our red Chl assignments with those of other groups. Our semiempirical calculations, which include the effects of Chl orientation, geometric distortions, excitonic coupling, charge-transfer interactions, and protein effects, suggest the following for the red Chls: Chls A32−B07, B24−B25, and A26−A27. All studies we are aware of suggest Chls A32−B07 to be red chlorophyll candidates. Jordan et al.,[1] based on distances between Mg centers and interplanar distances, suggested that Chls A38−A39, B37−B38, and B31−B32−B33 could also be responsible for the red absorption.

Based on semiempirical PPP calculations of the couplings, Sener et al.[48] suggests Chls A32−B07, A33−A34, A24−A35, and B22−B34 to be the red Chls. However, only excitonically coupled Chls were considered as candidates in their calculation. Their calculations also neglected protein interactions and coupling to charge-transfer states.

Assignments based on fitting spectra and dynamics[46] also suggest Chls A32−B07 to be red. In addition, Chls A38−A39 and B37−B38 were also suggested. They speculated that Chls A12−A14 and B31−B32−B33 may or may not be candidates, depending on the transition energies of these chlorophylls. In both our ab initio and INDO/S calculations (Table 2), the energies of Chls B31, B32, and B33 are placed above the average, therefore we suggest they are not the red Chls.

Bridging Chls. Contrary to the results of Byrdin et al.,[46] no large population density was found on the "bridging" Chls A40 and B39. This is a strong indication that they do not serve as local gathering centers of excitation energy. To determine their role in energy transfer, energy transfer rates need to be calculated. The current work provides the necessary ingredients for the rate calculations, and such calculations will be presented

in a future publication.[49] Calculations by others (in which energies of Chls are either homogeneous, randomly assigned, or obtained from fitting spectra) have shown that removal of the linker Chls have little effect on the energy transfer times (single step, slowest transfer, and trapping times)[46,50] and on the quantum yields.[48,50] We will now speculate on the role of the bridging Chls based on the calculated Chl excitation energies and couplings.

The strongest coupling between a RC Chl and any other antenna Chl is between Chl EC-B3 of the B-branch and the bridging Chl B39 (located toward the trimerization region). In turn, the bridging Chl is strongly coupled to Chl B38. These Chls, together with other Chls relevant for this discussion are shown in Figure 2. The excitation energies of the three Chls are about the same. The direct coupling from Chl B38 to EC-B3 is about 1 order of magnitude weaker than the couplings B38−B39 and B39−EC-B3. Since transfer rates are proportional to the square of the coupling, differences of 1 order of magnitude in couplings will translate to differences of 2 orders of magnitude in rates. Thus, the optimum energy transfer from Chl B38, or probably other Chls located in the trimerization region, will likely involve the bridging Chl B39. Based on symmetry arguments, one may expect Chl A40 to bridge energy transfer from Chls located on the other side of the trimerization region to the RC Chls.

Due to the large number of Chls in PS-I, it is difficult to make a general statement on whether the bridging Chls constitute the sole route of energy transfer into the RC. For example, the coupling of Chl EC-A1 is stronger to Chl A26 than to the bridge Chl A40, and symmetrically, the coupling of Chl EC-B1 is stronger to Chl B24 than to Chl B39. Again, an analysis based on the master equation is required to gain further insight into this question.

Absorption Spectrum. The oscillator strength is a measure of optical absorption strength. The oscillator strength of an excitonic state $|\tilde{n}\rangle$ is related to its dipole strength $D_{\tilde{n}}$ and energy $\epsilon_{\tilde{n}}$ through the relationship

$$f_{\tilde{n}} = (8\pi^2 mc\epsilon_{\tilde{n}}/3h^2)D_{\tilde{n}} \qquad (14)$$

Normalized dipole strengths for the 96 excitonic levels of the effective Hamiltonian (eqs 2, 3) are shown as a stick spectrum in Figure 6.

To simulate the absorption spectrum of PS-I at low temperatures, we have accounted for the effect of inhomogeneous broadening. Inhomogeneous broadening is usually treated as Gaussian distributed disorder in excitation energies.

We have thus generated a sample of 1000 random effective Hamiltonians $\hat{H}^r$, $r = 1, ..., 1000$. The diagonal matrix elements of each $\hat{H}^r$ ($\epsilon_1{}^r$, $\epsilon_2{}^r$, ..., $\epsilon_{96}{}^r$) no longer assume the values determined from our calculations (ϵ_1, ϵ_2, ..., ϵ_{96}). Now each $\epsilon_i{}^r$ is chosen from the Gaussian distribution

$$p(\epsilon_i{}^r) = \frac{1}{\sqrt{2\pi}\sigma}\exp[-(\epsilon_i{}^r - \epsilon_i)^2/2\sigma^2] \qquad (15)$$

The width σ accounts for the observed spectral inhomogeneities from hole burning experiments (Γ_I) and corresponds to $\Gamma_I = 100\ \mathrm{cm}^{-1}$.[51]

Each of the 1000 random Hamiltonians $\hat{H}^r$ is then diagonalized, and its excitation energies and oscillator strengths determined. The resulting excitation energies weighted with their corresponding oscillator strengths are binned into 5 nm bins. The absorption spectrum calculated in such a way is compared to the experimental absorption spectrum in Figure 6. The widths

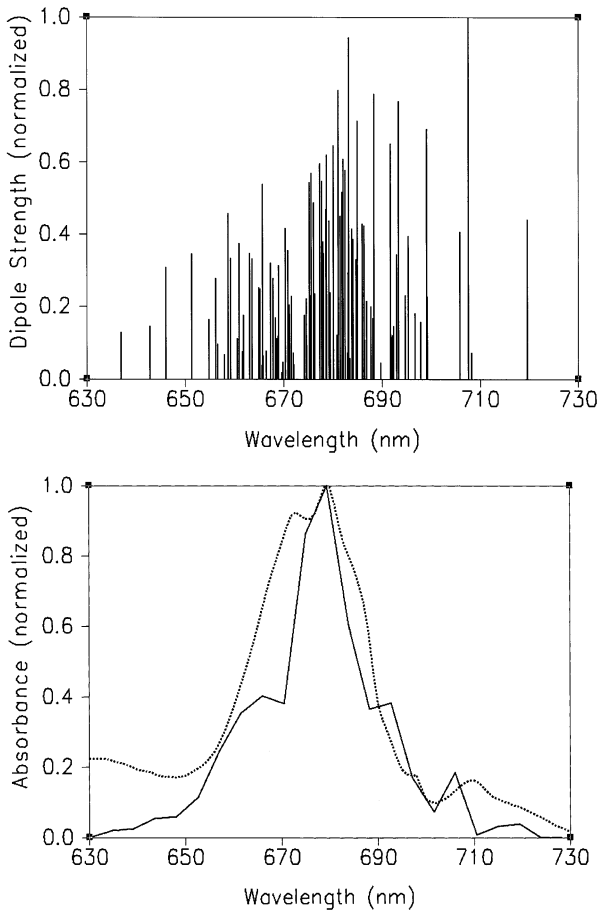

Figure 6. Chlorophyll Q_y region of the PS-I absorption spectrum; (top) stick spectrum of the effective Hamiltonian; (bottom) comparison of the experimental (dashed line) and the calculated (full line) absorption spectrum.

of our calculated spectrum is somewhat smaller that the width of the experimental spectrum. However, our calculated spectrum does not include homogeneous broadening, which is expected to further broaden the calculated spectrum. In addition, by inclusion of the homogeneous broadening the discrepancy on the blue side of the calculated and experimental spectra would most likely disappear.

Summary

We have determined, through the semiempirical INDO/S method, the excitation energies of 96 Chls and the couplings between closely separated chlorophylls in PS-I. Based on these calculations and an effective Hamiltonian description of chlorophyll Q_y excitations, we discuss the PS-I absorption spectrum and speculate on the location of the red chlorophylls.

Calculated Q_y excitation energies of the 96 Chls display significant spectral inhomogeneity. Calculations based on the crystal structure geometries performed in the absence of protein, water, and carotenoid residues yield a distribution of excitation energies with a standard deviation of 0.0203 eV (164 cm^{-1}). The difference in calculated excitation energies stems from a difference in Chl geometries induced by interactions with the protein surroundings.

When neighboring protein, water and carotenoid residues, are included in the INDO/S calculations, the differences in excitation energies are enhanced, resulting in a distribution with a standard deviation of 0.0304 eV (245 cm^{-1}). Charged and aromatic protein residues have a strong influence on the excitation

energies, inducing spectral shifts of up to 18 nm. Carotenoid molecules produce only slight shifts in excitation energies.

Additional spectral shifts occur in dimers or trimers of closely separated Chls, due to excitonic and charge resonance interactions. The latter two effects, combined, were determined to cause spectral shifts of up to 24 nm. Interestingly, protein residues are found to have a strong influence on the value of the charge−resonance interactions.

The effective Hamiltonian description accounts simultaneously for spectral shifts induced by interactions between Chls and their neighboring protein, water, or carotenoid residues, as well as by Chl−Chl interactions. This model is therefore well-suited to describe the PS-I absorption spectrum. The calculated absorption spectrum is in reasonable agreement with the experimental spectrum, considering the fact that the calculated spectrum does not include homogeneous broadening.

The excitonic state associated with the P700 heterodimer was, due to the calculated low excitation energy of P_A, determined to lie below the red Chls. An ab initio calculation gave a very similar result to the INDO/S method regarding the location of the P_A excitation energy, and there was a rather good agreement between the INDO/S and ab initio calculated distribution of excitation energies. A systematic investigation of the factors giving rise to the red shift of P_A in our calculation is necessary before a definitive statement can be made as to the origin of this shift. In case of a small number of Chls, additional errors might be introduced due to uncertainty in the protonation state of ionizable protein residues and due to the criteria for inclusion of protein residues in our calculations.

On the basis of the calculated eigenenergies of the effective Hamiltonian, we speculate on the location of the red chlorophylls. The red chlorophylls absorbing at 719 nm, believed to be located toward the trimerization region could be a tetramer of Chls A31, A32, B06, and B07. The red chlorophylls absorbing at 715 nm could be a dimer of Chls B24 and B25, and possibly due to symmetry analysis, the 708 nm Chls could be a dimer A26−A27.

Acknowledgment. We are grateful to Marshall G. Cory and Juha Linnanto for useful discussions on the INDO/S method, Xanthipe Jordanides for discussions on the TDC method, and Bas Gobets for sending us the data for the experimental absorption spectrum. All the figures except Figure 6 were produced with the program VMD.[52] This work was supported by the Director, Office of Science, Office of Basic Energy Sciences, Chemical Sciences Division of the U.S. Department of Energy under Contract No. DE-AC03-76SF00098.

References and Notes

(1) Jordan, P.; Fromme, P.; Witt, H. T.; Klukas, O.; Saenger, W.; Krauβ, N. *Nature* **2001**, *411*, 909.

(2) Guergova-Kuras, M.; Boudreaux, B.; Joliot, A.; Joliot, P.; Redding, K. *Proc. Natl. Acad. Sci. U. S. A.* **2001**, *98*, 4437.

(3) Yang, F.; Shen, G.; Schluchter, W. M.; Zybailov, B. L.; Ganago, A. O.; Vassiliev, I. R.; Bryant, D. A.; Golbeck, J. H. *J. Phys. Chem. B* **1998**, *102*, 8288.

(4) Watanabe, T.; Kobayashi, M.; Hongu, A.; Nakazato, M.; Hiyama, T. *FEBS Lett.* **1985**, *235*, 252.

(5) Watanabe, T.; Hongu, A.; Honda, K.; Nakazato, M.; Konno, M.; Saitoh, S. *Anal. Chem.* **1984**, *56*, 251.

(6) Schubert, W. D.; Klukas, O.; Krauss, N.; Saenger, W.; Fromme, P.; Witt, H. T. *J. Mol. Biol.* **1997**, *272*, 741.

(7) Gibasiewicz, K.; Ramesh, V. M.; Lin, S.; Redding, K.; Woodburry, N. W.; Webber, A. N. Mutations of ligands to connecting chlorophylls perturbs excitation dynamics in the core antenna of PSI from *chlamydomonas reinhardtii*. In *PS2001 Proceedings*: *12th International Congress on Photosynthesis*. CSIRO Publishing: Melbourne, Australia, 2001.

(8) Pullerits, T.; Sundström, V. *Acc. Chem. Res.* **1996**, *29*, 381.

(9) Fleming, G. R.; van Grondelle, R. *Curr. Opinion Struct. Biol.* **1997**, *7*, 738.

(10) Hu, X.; Damjanović, A.; Ritz, T.; Schulten, K. *Proc. Natl. Acad. Sci. U. S. A.* **1998**, *95*, 5935.

(11) Kennis, J. T. M.; Gobets, B.; van Stokkum, I. H. M.; Dekker: J. P.; van Grondelle, R.; Fleming, G. R. *J. Phys. Chem. B* **2001**, *105*, 4485.

(12) Melkozernov, A. N.; Lin, S.; Blankenship, R. E.; Valkunas, L. *Biophys. J.* **2001**, *81*, 1144.

(13) Gobets, B.; van Stokkum, I. H. M.; Rogner, M.; Kruip, J.; Schlodder, E.; Karapetyan, N. V.; Dekker, J. P.; van Grondelle, R. *Biophys. J.* **2001**, *81*, 407.

(14) Zazubovich, V.; Matsuzaki, S.; Johnson, T. W.; Hayes, J. M.; Chitnis, P. R.; Small, G. J. *J. Chem. Phys.* **1998**, *108*, 7763.

(15) Trissl, H. W.; Hecks, B.; Wulf, K. *Photochem. Photobiol.* **1993**, *57*, 108.

(16) Palsson, L.-O.; Flemming, C.; Gobets, B.; van Grondelle, R.; Dekker: J. P.; Schlodder, E. *Biophys. J.* **1998**, *74*, 2611.

(17) Palsson, L. O.; Dekker: J. P.; Schlodder, E.; Monshouwer, R.; van Grondelle, R. *Photosynth. Res.* **1996**, *48*, 239.

(18) Rätsep, M.; Johnson, T. W.; Chitnis, P. R.; Small, G. J. *J. Phys. Chem. B.* **2000**, *104*, 836.

(19) Tretiak, S.; Middleton, C.; Chernyak, V.; Mukamel, S. *J. Phys. Chem. B* **2000**, *104*, 4519.

(20) Knox, R. S. Dipole strengths in Chlorophyll-a and Bacteriochlorophyll-a. In *PS2001 Proceedings*: *12th International Congress on Photosynthesis;* CSIRO Publishing: Melbourne, Australia, 2001.

(21) Kleima, F. J.; Hofmann, E.; Gobets, B.; van Stokkum, I. H. M.; van Grondelle, R.; Diederichs, K.; van Amerongen, H. *Biophys. J.* **2000**, *78*, 344.

(22) Krueger, B. P.; Scholes, G. D.; Fleming, G. R. *J. Phys. Chem. B* **1998**, *102*, 5378.

(23) Damjanović, A.; Ritz, T.; Schulten, K. *Phys. Rev. E* **1999**, *59*, 3293.

(24) Ritz, T.; Damjanović, A.; Schulten, K.; Zhang, J.; Koyama, Y. *Photosynth. Res.* **2001**, *66*, 125.

(25) Hu, X.; Ritz, T.; Damjanović, A.; Schulten, K. *J. Phys. Chem. B* **1997**, *101*, 3854.

(26) Alden, R. G.; Johnson, E.; Nagarajan, V.; Parson, W. W.; Law, C. J.; Cogdell, R. G. *J. Phys. Chem. B* **1997**, *101*, 4467.

(27) Cory, M. G.; Zerner, M. C.; Hu, X.; Schulten, K. *J. Phys. Chem. B* **1998**, *102*, 7640.

(28) Scholes, G. D.; Gould, I. R.; Cogdell, R. J.; Fleming, G. R. *J. Phys. Chem. B* **1999**, *103*, 2543.

(29) Linnanto, J.; Korppi-Tommola, J. E. I.; Helenius, V. M. *J. Phys. Chem. B* **1999**, *103*, 8739.

(30) Ridley, J.; Zerner, M. *Theor. Chim. Acta* **1973**, *32*, 111.

(31) Zerner, M.; Loew, G.; Kirchner, R.; Mueller-Westerhoff, U. *J. Am. Chem. Soc.* **1980**, *102*, 589.

(32) Brünger, A. T. *X-PLOR, Version 3.1*: *A System for X-ray Crystallography and NMR*. The Howard Hughes Medical Institute and Department of Molecular Biophysics and Biochemistry, Yale University, 1992.

(33) Stewart, J. J. P. *J. Comput. Chem.* **1989**, *10*, 209.

(34) Frisch, M. J.; Trucks, G. W.; Schlegel, H. B.; Scuseria, G. E.; Robb, M. A.; Cheeseman, J. R.; V. G. Zakrzewski, J. A. M.; Stratmann, R. E.; Burant, J. C.; S. Dapprich, J. M. M.; Daniels, A. D.; Kudin, K. N.; Strain, M. C.; O. Farkas, J. T.; Barone, V.; Cossi, M.; Cammi, R.; Mennucci, B.; C. Pomelli, C. A.; Clifford, S.; Ochterski, J.; Petersson, G. A.; P. Y. Ayala, Q. C.; Morokuma, K.; Malick, D. K.; Rabuck, A. D.; K. Raghavachari, J. B. F.; Cioslowski, J.; Ortiz, J. V.; Stefanov, B. B.; Liu, G.; Liashenko, A.; Piskorz, P.; Komaromi, I.; Gomperts, R.; R. L. Martin, D. J. F.; Keith, T.; Al-Laham, M. A.; Peng, C. Y.; A. Nanayakkara, C. G.; Challacombe, M.; Gill, P. M. W.; Johnson, B. G.; W. Chen, M. W. W.; Andres, J. L.; Head-Gordon, M.; Replogle, E. S.; Pople, J. A. *Gaussian 98, Revision A7*; Gaussian Inc.: Pittsburgh, PA, 1998.

(35) Thompson, M.; Zerner, M. *J. Am. Chem. Soc.* **1991**, *113*, 8210.

(36) Thompson, M.; Zerner, M. C.; Fajer, J. *J. Phys. Chem.* **1991**, *95*, 5693.

(37) Hsu, C.-P.; Walla, P. J.; Head-Gordon, M.; Fleming, G. R. *J. Phys. Chem. B* **2001**, *105*, 11016.

(38) Fowler, G.; Sockalingum, G.; Robert, B.; Hunter, C. *Biochem. J.* **1994**, *299*, 695.

(39) Gall, A.; Fowler, G. J. S.; Hunter, C. N.; Robert, B. *Biochemistry* **1997**, *36*, 16282.

(40) Witt, H.; Schlodder, E.; Teutloff, C.; Carbonera, D.; Niklas, J., and Lubitz, W. Site-directed mutagenesis of Thr A739 of photosystem I in *chlamydomonas reinhardtii* alters significantly the excitonic and electronic coupling of the primary electron donor P700. In *PS2001 Proceedings*: *12th International Congress on Photosynthesis*; CSIRO Publishing: Melbourne, Australia, 2001.

(41) Hanson, L. K.; Fayer, J.; Thompson, M. A.; Zerner, M. C. *J. Am. Chem. Soc.* **1987**, *109*, 4728.

(42) Hsu, C.-P.; Fleming, G. R.; Head-Gordon, M.; Head-Gordon, T. *J. Chem. Phys.* **2001**, *114*, 3065.

(43) Thompson, M. A.; Zerner, M. C.; Fajer, J. *J. Phys. Chem.* **1990**, *94*, 3820.
(44) Meier, T.; Zhao, Y.; Chernyak, V.; Mukamel, S. *J. Chem. Phys.* **1997**, *107*, 3876.
(45) Damjanović, A.; Kosztin, I.; Kleinekathoefer, U.; Schulten, K. *Phys. Rev. E* **2002**, *65*, 031919.
(46) Byrdin, M.; Jordan, P.; Krauss, N.; Fromme, P.; Stehlik, D.; Schlodder, E. *Biophys. J.* **2002**, *83*, 433.
(47) Small, G. J. *Chem. Phys.* **1995**, *197*, 239.
(48) Sener, M. K.; Lu, D.; Ritz, T.; Park, S.; Fromme, P.; Schulten, K. *J. Phys. Chem. B* **2002**, *106*, 7948.
(49) Damjanović, A.; Vaswani, H. M.; Yang, M.; Fleming, G. R. Manuscript in preparation.
(50) Gobets, S. Ph.D. Thesis.
(51) Raja, N.; Reddy, S.; Lyle, P. A., and Small, G. J. *Photosynth. Res.* **1992**, *31*, 167.
(52) Humphrey, W.; Dalke, A.; Schulten, K. *J. Mol. Graphics* **1996**, *14*, 33.